

Silicon Surface Nanostructuring for Covalent Immobilization of Biomolecules

Celia Rogero,^{*,†,‡} Benjamin T. Chaffey,[§] Eva Mateo-Martí,[†] Jesús M. Sobrado,[†] Benjamin R. Horrocks,[‡] Andrew Houlton,[‡] Jeremy H. Lakey,[§] Carlos Briones,[†] and José A Martín-Gago^{†,||}

Centro de Astrobiología (CSIC-INTA), Carretera de Ajalvir, Km. 4, 28850 Torrejón de Ardoz, Madrid, Spain, Chemical Nanoscience Laboratories, School of Natural Sciences, The University of Newcastle-upon-Tyne, Newcastle-upon-Tyne, NE1 7RU, Great Britain, The Institute of Cellular and Molecular Biosciences, The Medical School, The University of Newcastle-upon-Tyne, Newcastle-upon-Tyne, NE2 4HH, Great Britain, and Instituto de Ciencia de Materiales de Madrid (CSIC), Sor Juana Inés de la Cruz, 28049 Madrid, Spain

Received: February 21, 2008; Revised Manuscript Received: March 31, 2008

We present a straightforward strategy to control the average distance of immobilized biomolecules on silicon surfaces. We exploit the reaction taking place between the amino residues within the biomolecules (lysine groups of proteins or the N-terminus of oligomers of peptide nucleic acid, PNA) and the aldehyde-terminated groups presented in a mixed aldehyde/alkyl organic monolayer on a silicon surface. The mixed monolayers were prepared by a thermal reaction of hydrogen-terminated Si(111) with a mixture of undecene and undecenyl-aldehyde. We quantitatively evaluate the surface concentration of aldehyde in the monolayer by atomic force microscopy and an intensity analysis of core level X-ray photoemission spectroscopy peaks. These complementary techniques show that the surface density of the reactive terminal groups reflects the mole fraction of aldehyde in the reactive solution used to modify the silicon surface. The further immobilization of proteins or peptide nucleic acids on the monolayer shows that the density of biomolecules reproduces the aldehyde surface density, which indicates a specific covalent attachment and a negligible nonspecific adsorption. The proposed procedure makes possible to control the average distance of the immobilized active biomolecules on the silicon surface, which could be of great relevance for applications in the interdisciplinary field of biosensors.

Introduction

There is growing interest in gaining information on the mechanisms controlling the self-assembly of biomolecules in spatially defined areas of a surface, due to its possible application in biosensor technology.^{1–6} Although current microarray technology makes use of glass substrates and fluorescence detection techniques, fundamental studies are being performed on a wide range of substrates including metals (mainly on gold^{7–9}), oxides,^{10–12} or semiconductors. These alternative surfaces are particularly important because they allow the use of electronic detection methods. Over the past decade, the formation of organic self-assembled monolayers (SAMs) on oxide-free silicon surfaces has attracted a lot of attention.^{13,14} The first reason for such interest is that it is possible to obtain well-ordered, functionalized monolayers on the hydrogen-terminated silicon surfaces, thanks to the robust Si–C bond that allows covalent immobilization of a wide range of biological entities including amino acids, proteins, and nucleic acids. The second advantage of this strategy is that, since the Si–C bond is irreversible, it is possible to form mixed monolayers with organic molecules exposing reactive and nonreactive terminal groups that allow a further immobilization of biomolecules with a controlled spatial

separation. Finally, it is possible to combine these mixed SAMs with existing silicon technology for applications in electronics and micromachining.

Many different biomolecules have been successfully immobilized on Si surfaces, among them glyoxylyl-modified peptides,¹⁵ saccharides,^{16,17} and nucleic acids. DNA molecules have been immobilized on the silicon surface by conjugation to an amine-modified Si surface.^{18–20} Alkyl monolayers terminated in carboxylic or alcohol groups were also used for the coupling of amino acids or DNA on Si surfaces using standard amide coupling protocols.²¹ Alternatively, single-stranded (ss) DNA or ferrocenyl-modified oligonucleotides have been also directly synthesized at an alcohol-functionalized silicon surface.^{22,23} Nevertheless, these strategies require an initial attachment of protected alkyl chains and their subsequent deprotection by acid or base hydrolysis after the surface functionalization. In many cases, the reaction conditions for deprotection result in surface damage. Therefore, alternative simple and mild approaches are of interest for the immobilization of chemical and biological molecules on semiconductor surfaces.

Voicu and co-workers have described a direct method for anchoring terminal carboxylic acid functions on Si surfaces, presenting a significant advance in the preparation of silicon surfaces for the incorporation of biomolecules.²⁴ An alternative to this procedure is the use of aldehyde-modified Si surfaces, since the aldehyde group can covalently bind proteins or peptides by reaction with the amine group present on their lysine residues. The aldehyde group has been previously used to generate protein microarrays on glass slides.²⁵ However, it has been reported that under thermal reaction conditions, the aldehyde groups react

* To whom correspondence should be addressed. E-mail: rogerobc@inta.es. Phone: 0034915201042. Fax: 003491520107.

[†] Centro de Astrobiología.

[‡] Chemical Nanoscience Laboratories, School of Natural Sciences, The University of Newcastle-upon-Tyne.

[§] The Institute of Cellular and Molecular Biosciences, The Medical School, The University of Newcastle-upon-Tyne.

^{||} Instituto de Ciencia de Materiales de Madrid.

with the surface to form Si-O-C bonds²⁶ that prevent a further biomolecule attachment. At first sight, the use of difunctional vinyl aldehydes does not look promising as a route to the controlled preparation of monolayers suited to immobilization via Schiff base chemistry. However, we show here that this is not the case. We have found that the thermal reaction of undecenyl-aldehyde with Si (111)-H produces a monolayer bearing sufficient unreacted aldehyde groups to facilitate the further attachment of either proteins or the nucleic acid analogue PNA by a simple Schiff base coupling reaction in aqueous solution. We also found that the use of a mixture of undecenyl-aldehyde and undecene allows us to control the density of immobilized biomolecules and to limit their nonspecific adsorption. Different surface characterization techniques have been used to obtain these results. Particularly, X-ray photoelectron spectroscopy (XPS) allows us to obtain a direct relation between the ratio of the alkenylic aldehyde in the solution during the thermal reaction and the final amount of detected immobilized biomolecules. Additionally, atomic force microscopy (AFM) provides a description of the topography of the molecular layer. Fluorescence microscopy confirms that the structure of the proteins remains intact after their immobilization, as shown by the attachment of green fluorescent protein (GFP): the maintenance of its intense fluorescence is a clear fingerprint of the preservation of its functional structure upon binding to the modified Si surface.

Experimental Details

H-Terminated Silicon Wafers. Single crystal silicon samples were cut from (111)-oriented wafers (miscut angle $<0.1^\circ$) to a size of ca. $1 \times 1 \text{ cm}^2$ using a diamond pencil. These chips were degreased in boiling trichloroethylene for 30 min, followed by acetone for 5 min, isopropanol for 5 min, and a thorough rinse with ultrapure water. An oxide layer was then grown in freshly prepared piranha solution (4:1 v/v concentrated H_2SO_4 and 30% H_2O_2) for 15 min at 80°C . The chips were then removed, washed thoroughly with water, and transferred to a sealed Teflon etching cell containing semiconductor-grade NH_4F (40%). The NH_4F etchant was degassed by purging with argon for 1 h prior to the immersion of the chips. The chips were etched for 30 min in the solution at an orientation of 45° with the polished side facing down, under an atmosphere of argon. After removal from the etchant, the wafers were rinsed with water for few seconds and dried by wicking with filter paper.

Mixed Monolayer Preparation. The hydrogen-terminated silicon chips were transferred to Schlenk flasks containing 8 mL of a 20 mM solution of the appropriate molar ratio of the two molecular compounds that will form the mixed SAM, undecene (denoted C_{11} below) and undecenyl aldehyde (denoted C_{10}CHO), diluted in dry solvent (toluene), and placed under dry N_2 . After 18 h at reflux (toluene bp = 110.6°C), the wafers were rinsed with dichloromethane, acetone, and finally water before being dried by wicking with filter paper.

Protein TolAIII-GFP Attachment. TolAIII-GFP was selected as a model protein for these experiments as it is readily expressed and purified in large quantities, being soluble and stable in a wide variety of buffer conditions. The incorporation of GFP in the recombinant protein allowed rapid and straightforward qualitative assessment of the degree of protein immobilization on the surfaces by fluorescent microscopy and also indicated whether the immobilization strategy had severe detrimental effects on protein structure and function (since denatured GFP will no longer fluoresce).

Protein (TolAIII-GFP, 10 mg/ml) was prepared by first cloning the GFP gene sequence into the pTol-T vector.²⁷ The resulting recombinant protein was expressed in *E. coli* and purified to homogeneity by immobilized Ni^{2+} ion affinity chromatography followed by size-exclusion chromatography. Protein purity was confirmed by the presence of a single band on a Coomassie blue stained reducing sodium dodecylsulfate polyacrylamide gel electrophoresis gel.

Purified TolAIII-GFP molecules were immobilized by incubation at 0.5 mg/ml with the $\text{C}_{10}\text{CHO}:\text{C}_{11}$ -modified silicon surface (approximately 1 cm^2) in 100 μL of phosphate-buffered saline (PBS), mixed with 0.1 M sodium cyanoborohydride, NaCNBH_3 . The immobilization took place for 1–2 h at room temperature. Although Schiff base chemistry is reversible at neutral pH, we found that the well-known technique of reducing the transient imine linkage by cyanoborohydride can be applied in a one-pot reaction to render the linkage to the surface irreversible. After reaction the chips were rinsed with PBS and any remaining aldehyde was quenched by addition of 100 mM ethanolamine/0.1 M NaCNBH_3 in PBS for 2 h. To minimize any nonspecific physical adsorption of proteins, the chips were extensively washed with high salt (1 M NaCl) PBS and finally PBS before use.

PNA Immobilization. PNA is a synthetic nucleic acid analogue that combines nucleic acid features with a peptidic linear backbone, being a neutral and achiral molecule capable of strongly and specifically binding to complementary DNA (cDNA).^{28,29} We have used the ssPNA oligomer PG142 (with sequence, written from the amino to the carboxyl termini, AATCCCCGCAT). This sequence was chosen for its relevance in virology since it contains the sequence corresponding to a highly antigenic region of the capsid protein VP1 of the animal pathogen foot-and-mouth disease virus (FMDV).³⁰

The immobilization was carried out by placing a 20- μL drop of PNA solution (5 μM in milli-Q grade water) on a Si chip ($1 \times 1 \text{ cm}$) with a $\text{C}_{10}\text{CHO}:\text{C}_{11}$ -bearing surface. Immediately, 20 μL of a reducing solution was added to the PNA drop. This reducing solution was prepared by mixing 1 mL of citrate buffer and 20 μL of 5.0 M aqueous sodium of NaCNBH_3 . Since ssPNA is highly stable in water and it is an apolar molecule, immobilization could take place without involving any salt or buffer. However, the use of a buffer solution was necessary to reduce the pH of the NaCNBH_3 since basic solutions act as etchant on the Si surfaces. Citrate buffer was used instead of PBS in order to avoid compounds containing phosphorus, since in further experiments we will try to hybridize the immobilized ssPNA oligomers with the cDNA chains, being the P atoms of DNA used as a fingerprint of the hybridization process (the characterization of the PNA/DNA hybridization process will be the subject of a separate paper). The solution was left to react for 18 h (humid chamber, fume cupboard). The surface was vigorously rinsed with ultrapure water with agitation after reaction.

Characterization of the Modified Surfaces. XPS experiments were performed at room temperature (RT) in an ultrahigh vacuum (UHV) system equipped with a hemispherical electron energy analyzer. Spectra were measured using Mg K α X-rays as the excitation source. Si2p, C1s, O1s, and N1s were measured, within an overall resolution estimated to be around 0.7 eV. All spectra were normalized to the Si2p peak. Because the N signal comes exclusively from the biomolecules, TolAIII-GFP and ssPNA, the N1s core level peak will scale with the efficiency of the immobilization process. No other extra XPS peaks coming from the solvents, the buffer reactants, or the

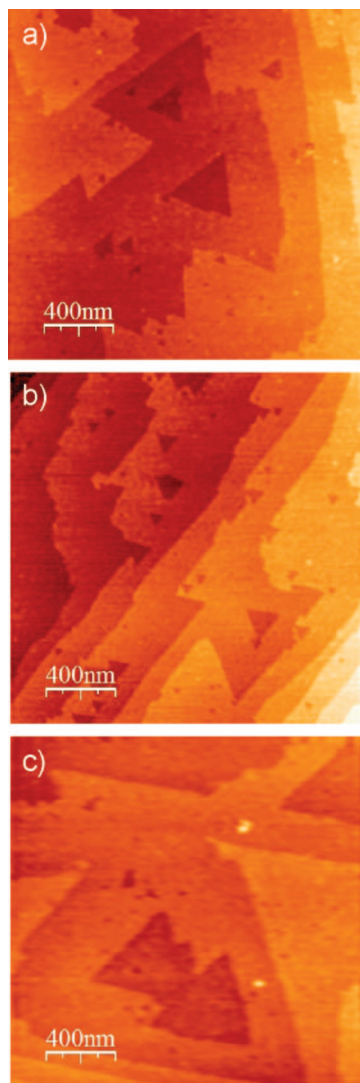


Figure 1. AFM images of three Si surfaces prepared using different $C_{10}CHO:C_{11}$ solution ratios: (a) 100:0; (b) 50:50; (c) 10:90.

sodium cyanoborohydride have been detected, indicating that solution was completely removed after the immobilization.

AFM images were collected in air with two different microscopes: Nanoscope IIIa multimode instrument (Veeco, Metrology group) and Nanotec Electronica microscope.³¹ Two different tips were used: (1) 125- μm long, 35- μm wide silicon cantilevers with a typical force constant of 40 N m^{-1} and a resonant frequency of 325 kHz; (2) 100- μm long, 36- μm wide Si_3N_4 gold-coated cantilevers with a nominal force constant of 0.12 N m^{-1} .

Fluorescence images were obtained using a Leica DM LB microscope fitted with a SPOT RT KE camera. The captured images were analyzed using the SPOT Advance software package. To monitor the fluorescence of immobilized GFP molecules on a surface, near-UV excitation light was used in reflective illumination mode and emission in the green wavelength range monitored.

Results and Discussion

Mixed monolayers on the Si (111)-H surface were formed by a thermal alkylation reaction with a mixture of undecenyl aldehyde ($C_{10}CHO$) and undecene (C_{11}). Figure 1 shows the (2 $\mu\text{m} \times 2 \mu\text{m}$) AFM images for three different surface $C_{10}CHO:C_{11}$ ratios (100:0, 50:50, and 10:90). Independent of the

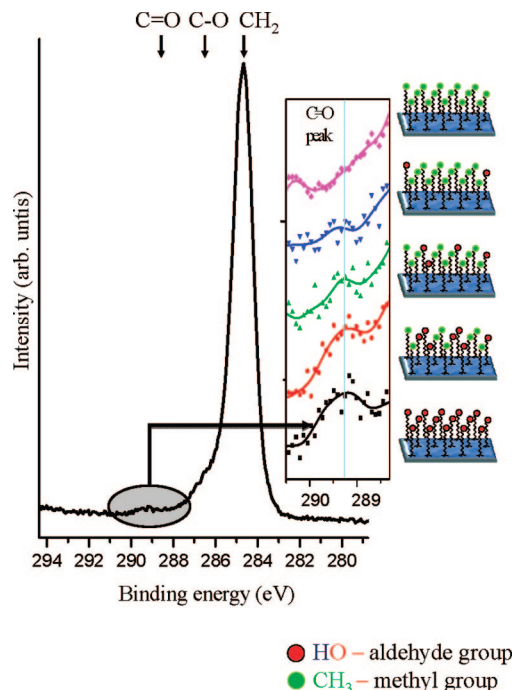


Figure 2. C_{1s} core level XPS peak corresponding to a 100:0 $C_{10}CHO:C_{11}$ solution. Zoom of the C=O C_{1s} core level curve component recorded for five different surface concentrations ($C_{10}CHO:C_{11}$ ratios of 0:100, 0.01:99.99, 10:90, 50:50, 100:0).

$C_{10}CHO:C_{11}$ ratio, all the surfaces retain the morphological features observed for the clean Si (111)-H surface: flat terraces separated by monatomic steps. This suggests that the surface is uniformly covered by the molecular film. The step height between two adjacent terraces was 3.3 \AA , which is in reasonable agreement with the value of 3.14 \AA for a monatomic step derived from the crystal structure of Si. Apparently, the two components of the mixed film are homogeneously distributed on the surface, in good agreement with the previous studies for other mixed monolayers.^{17,21,32,33} However, the AFM analysis cannot discriminate their bonding with the Si surface, i.e., whether the aldehyde alkene chains have reacted with the surface breaking the C=C bond (forming a Si-C bond) or by the aldehyde-terminated group (forming a Si-O-C bond) as it has been reported to happen in some cases.²⁶

This question can be addressed by XPS. Thus, an analysis of the C_{1s} core level XPS spectra measured for different surface concentrations was performed in order to learn more about the chemical interactions at the silicon-monolayer interface. Figure 2 shows the C_{1s} core level spectra measured for a 100:0 $C_{10}CHO:C_{11}$ surface. Very similar line shapes were observed for the five cases that were analyzed ($C_{10}CHO:C_{11}$ ratios of 0:100, 0.01:99.99, 10:90, 50:50, 100:0). For all these spectra, it is possible to decompose the C_{1s} core level photoemission peak into curve components and isolate the components related solely to the presence of the aldehyde group in the outermost part of the monolayer, i.e., those that have not reacted with the Si surface.

The overall line shapes of the XPS spectra are well fitted by three components. The first and most intense one, centered at 284.5 eV, can be assigned to the $-\text{CH}_2-$ group in the alkyl chain and also, potentially, to some air contamination.^{15,34,35} The second one, centered at 286 eV, is related to $-\text{C}-\text{O}$ bonds. Finally, the third component at 289.4 eV is associated with $-\text{C}=\text{O}$ (see Figure 2, insert). It is difficult to determine whether the component at 286 eV is related to the presence of Si-O-C

TABLE 1: Calculated Mole Fractions of Aldehyde-Terminated groups in the Monolayer Determined by XPS and Nominal Mole Fractions of Aldehyde Chains in the Reaction Solutions

aldehyde mole fraction in the monolayer	nominal aldehyde mole fraction in the solution
100%	100%
57%	50%
15%	10%
0%	0.01%
0%	0%

bonds at the interface from reaction of the aldehyde group with Si-H bonds or is related to oxidation (induced by some kind of contamination during the thermal process) and, therefore, independent of the presence of the aldehyde group. Fortunately, the small third component cannot be related to contamination and it is an indication of the presence of aldehyde groups on the topmost part of the modified surface, i.e., far from the Si interface. In fact, although the line shapes for the five spectra are similar, it is possible to distinguish intensity variations of this last component as can be observed in Figure 2: the lower the nominal aldehyde solution concentration, the lower the $-C=O$ component intensity. Although the XPS intensity of the aldehyde contribution is very low, it is possible to quantitatively analyze the evolution of the integrated intensity of this C1s component with respect to the contribution coming from the main peak component (related to the total number of alkyl chains). Table 1 shows the values of these calculated mole fractions of aldehyde terminated groups in the monolayer compared to the nominal mole fractions of aldehyde chains in the reaction solutions. These monolayer mole fractions were calculated by using the ratio $A_{(-C=O)}/A_{(CH_2)}$ (where $A_{(-C=O)}$ is the intensity of the component associated with $-C=O$ and $A_{(CH_2)}$ the contribution coming from the C-C bond in the chain) for each of the five prepared surfaces normalized by the same intensity ratio ($A_{(-C=O)}/A_{(CH_2)}$) calculated for the pure $C_{10}CHO$ monolayer. This shows that while some Si-O-C bonding is likely to be present at the surface (induced by reaction of the aldehyde group under the reaction conditions), the concentration of unreacted aldehyde groups at the top face of the monolayer is proportional to the mole fraction of $C_{10}CHO$ in the solution.

This simple experimental procedure enables the density of aldehyde groups on the surface to be controlled, and, potentially, also enables control over the density of immobilized biomolecules on a nanometer scale. To test this hypothesis, either proteins or ssPNA chains were immobilized using different ratios of undecene and undecyl aldehyde. These amino-containing biomolecules covalently bond to the aldehyde groups by a Schiff base reaction. Although the reaction with the aldehydes of either the lysine residues of proteins or the N-terminus of ssPNA is reversible, it can be fixed by reduction using NaCNBH₃ in a "one-pot" reaction in aqueous solution. On the basis of our previous experiments with lysine and urea,³⁶ we first studied the immobilization of the protein TolAIII-GFP to the mixed surfaces. With a $C_{10}CHO$ -modified surface (100:0 $C_{10}CHO:C_{11}$), the surface was fully covered by TolAIII-GFP, as can be seen in Figure 3a. The surface morphology has become grainy, and the terrace structure is not visible any more. When the same protein is incubated on Si modified with only 1% of 1-aldehyde (1:99 $C_{10}CHO:C_{11}$), AFM images reveal that the silicon terrace structure is visible, and a few protrusions are observed (Figure 3b). The reduction in the density of these protrusions follows the decrease of aldehyde groups (reactive centers) in the modified Si surface. Fluorescence experiments

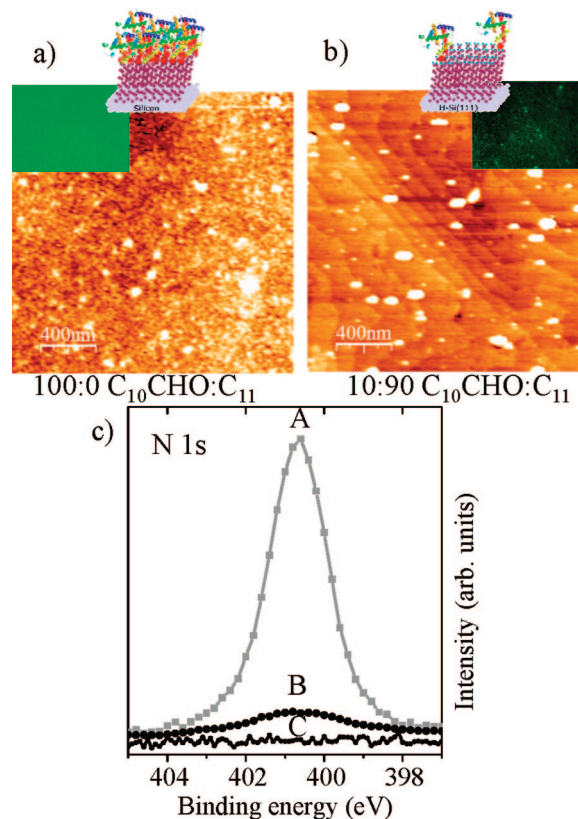


Figure 3. (a and b) AFM images of incubated TolAIII proteins on the nominal 100% aldehyde (100:0 $C_{10}CHO:C_{11}$) and 1% aldehyde modified surfaces. Inserted are the fluorescence experiment images of both surfaces. (c) N1s core level measured for the aforementioned surfaces for the 100:0 $C_{10}CHO:C_{11}$ (A) and for the 1:99 $C_{10}CHO:C_{11}$ (B) and also for the control surface of proteins incubated on a 0:100 $C_{10}CHO:C_{11}$ modified surface (C).

(insets to parts a and b of Figure 3) also reveal that images from the surfaces with fluorescence protein (GFP portion) attached to the 100:0 $C_{10}CHO:C_{11}$ layer are nearly homogeneously green and much brighter than the images from the surface with the proteins immobilized on 1:99 $C_{10}CHO:C_{11}$, where only discrete bright green spots are distinguished on a dark background. It is known that TolAIII-GFP is only fluorescent when the GFP portion is correctly folded, so both images provide evidences that the protein remains intact upon immobilization on any of the monolayers.

The XPS analysis reveals that a strong N1s signal is detected when the proteins are incubated on a 100:0 $C_{10}CHO:C_{11}$ modified silicon surface, providing an initial evidence of the presence of the proteins immobilized on the functionalized surface (spectrum labeled A in Figure 3c). The detection of the N1s core level peak on the XPS spectra directly reveals the presence of the biomolecules on the surface because only the proteins (and later the ssPNA) contain N atoms. The N1s signal is clearly reduced in intensity (spectrum labeled B in Figure 3c), as expected, when the incubation is performed on a surface prepared from a 1:99 $C_{10}CHO:C_{11}$ solution. Finally, when proteins are incubated on a 0% $C_{10}CHO$ (0:100 $C_{10}CHO:C_{11}$) modified surface, as a negative control experiment, no N1s signal is detected (spectrum labeled C in Figure 3c). Therefore, the presence of the protein on the surface can only be associated with the formation of a covalent bond between the amino groups of the protein and the aldehyde groups of the monolayer and not to the nonspecific adsorption or contamination by the NaCNBH₃ reagent.

These qualitative observations can be quantified to determine the amount of proteins on the surface and, as a consequence, the amount of reactive centers (aldehyde groups) on the mixed monolayer. From the analysis of the Figure 3b it is possible to obtain a value for $A_{\text{image}}/A_{\text{protrusions}} = 7$ (A_{image} is the total area of the image, and $A_{\text{protrusions}}$ is the area occupied by the protein protrusions). The approximate values for the footprints of one alkene chain and the TolAIII-GFP protein are of the order of 0.25³⁵ and 6 nm², respectively.³⁷ Therefore, we can calculate a protein density of 0.024. These values indicate that the composition of the surface is 0.6:99.4 C₁₀CHO:C₁₁. Although the result is slightly lower than the expected nominal 1% aldehyde concentration of the original solution, the value is within the experimental error. This simple calculation is valid assuming that there is only one aldehyde reactive group below one protein.

Moreover, the analysis of the XPS core level intensities also gives similar values. Aside from being the primary interest, the attachment of the biomolecules presents the advantage that it can be used for an indirect quantisation of available aldehyde groups on the surface. It is possible to determine the relative amounts of biomolecules on the surface by analyzing either the attenuation of the Si2p core level due to the attachment of the biomolecule or the N1s core level intensities for the different concentrations. By use of this last procedure we can compare the intensities of the two aforementioned N1s spectra (labeled A and B in the Figure 3c) and extract from these the density of proteins for the partially covered surface, because the photo-emission intensity is proportional to the number of proteins. Moreover, it is possible to determine the number of active centers on the mixed monolayers having taken into account the values for the footprints of one alkene chain and one TolAIII-GFP protein. Thus, defining I_X as the N1s core level intensity from the incubation performed on the surface prepared from a nominal 1:99 C₁₀CHO:C₁₁ solution (B spectrum) and $I_{100\%}$ as the N1s intensity from the incubation performed on the surface prepared from a 100:0 C₁₀CHO:C₁₁ solution (A spectrum), it is possible to calculate the ratio $I_X/I_{100\%}$ from the spectra and get a relationship of $I_{100\%} = 6.25I_X$. That means that for the partially covered surface there is only 1 protein in the area occupied by 6.25 when the entire surface has reacted. Since, in average, about 24 alkene chains are located below one protein, a 16% of protein coverage for the partially covered surface can be translated into a 0.7% aldehyde mixed monolayer (0.7:99.3 C₁₀CHO:C₁₁ mixed monolayer), in good agreement with the 1% aldehyde solution concentration having taken into account the experimental error and the uncertainty in the protein size estimation.

The second set of experiments performed involved the immobilization of the ssPNA chains on the mixed layer. Previous results showed that cysteine-modified ssPNA chains were successfully immobilized on gold surfaces, through the terminal thiol group of the biomolecule. Those studies revealed that the PNAs form a stable, ordered SAM in air, maintaining their DNA recognition capability.^{9,38,39} We have followed a different approach here, since we have used unmodified ssPNA chains that promote the reaction with aldehyde groups via the amino group of the terminal Lys of their peptidomimetic backbone.

The AFM images measured after 18 h of ssPNA immobilization reaction on the 100:0 C₁₀CHO:C₁₁ show again that the terraced surface is completely covered by a textured layer (Figure 4). In this case, ssPNA molecules consist of straight chains, about 4 nm long and 1.6 nm wide,^{9,38} that can therefore be oriented on the surface parallel or perpendicularly, meaning lying down or standing up. To learn which is the actual height

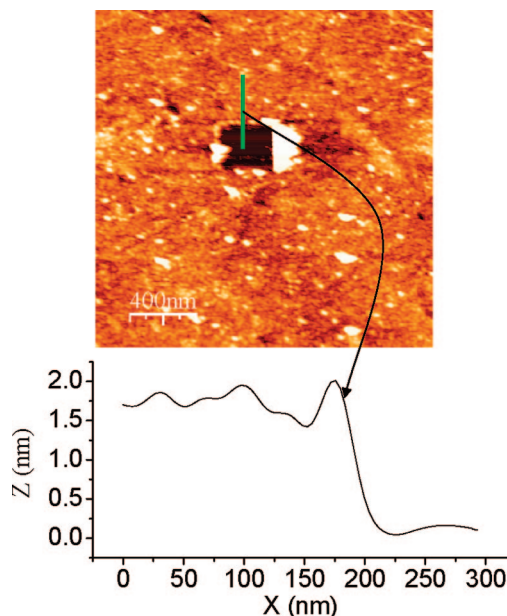


Figure 4. AFM image of incubated ssPNA oligomers on a nominal 100:0 C₁₀CHO:C₁₁-modified Si surface. The dark area corresponds to a place previously scanned applying high forces to remove the most external PNA layer. The profile indicates the height of the ssPNA layer.

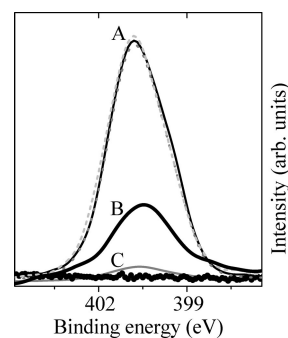


Figure 5. N1s core level XPS spectra after ssPNA incubated on the 100:0 C₁₀CHO:C₁₁-modified surface (black solid line in the group of spectra labelled as A), the 10:90 C₁₀CHO:C₁₁-modified surface (gray dotted line in the group of spectra labelled as A), the 5:95 C₁₀CHO:C₁₁-modified surface (gray dashed line in the group of spectra labelled as A), the 0.1:99.9 C₁₀CHO:C₁₁-modified surface (spectrum identified as B), the 0:100 C₁₀CHO:C₁₁-modified surface (spectrum identified as C), and the N1s core level measured on 100:0 C₁₀CHO:C₁₁ before incubation.

of the immobilized layer, we have made a square hole on the surface with the AFM tip. To perform this surface modification, we scanned over a square area applying a high force. Then, we have acquired images of the scratched area. The black area in Figure 4 corresponds to this area, in which we have swept out the PNA bilayer. Complementary experiments performed on the alkyl monolayer confirm that the mixed monolayer remains unchanged by such high forces and therefore the changes in height we discuss here are only ascribed to the immobilized biomolecules. The average height of the step (between the outermost PNA layer and the alkyl termination) is about 1.6 nm, as can be seen in the inserted profile in Figure 4. This small height indicates that ssPNA molecules are lying down on the surface.

Figure 5 shows the N1s core level spectra of this sample (black line labeled as A). Again, the detection of the N1s is a clear fingerprint of the presence of the ssPNA on the surface. When ssPNA was incubating on surfaces prepared from smaller

TABLE 2: Percentage of C, N, and O Atoms Extracted from the XPS Core Level for the ssPNA Molecules Incubated on the 100, 10, and 5% C₁₀CHO-Modified surfaces (Ratio of C, N, and O Atoms on the PNA Formula Is Also Included)

	nominal C ₁₀ CHO concentration			from the PNA formula
	100%	10%	5%	
C	69	66	67	53
N	18	22	15	34
O	13	12	18	13

nominal C₁₀CHO:C₁₁ ratios, 10:90 and 5:95, N1s core level photoelectrons were always detected (gray dotted and dashed lines in Figure 5). In fact, the N1s core level intensity is the same for the three cases. The three spectra maintain similar C:N:O increment ratios after immobilization (Table 2), which indicates that apparently the three immobilization experiments (with 100, 10, and 5% aldehyde) lead to the same concentration of ssPNA on the surface (for the quantitative calculation shown in Table 2, each peak intensity was divided by each relevant sensitivity factors, 0.25 for C1s, 0.42 for N1s, and 0.66 for O1s, and the ssPNA were calculated for the ssPNA oligomer PG142). The calculated values are in agreement with the ideal percentage of elements for one single layer of biomolecule on the modified surfaces. Although these nominal aldehyde surface concentrations were very useful for the determination of the formation of only one bimolecular layer on the modified silicon surfaces, they cannot help to discriminate whether the ssPNA are only bound to the reactive centers. The 5:95 C₁₀CHO:C₁₁ and the 100:0 C₁₀CHO:C₁₁ modified surfaces do not differ in the amount of ssPNA, because both can immobilize a complete monolayer of ssPNA, since the distance for reactive centers, even for the former, is shorter than the size of the ssPNA molecules.

To immobilize isolated ssPNA molecules, C₁₀CHO:C₁₁ ratios lower than 3.5% are required. The spectrum labeled B in Figure 5 shows the N1s core level photoemission peak for ssPNA incubated on a 0.1:99.9 C₁₀CHO:C₁₁ nominal surface. Clearly, its intensity is lower than the one obtained from the previous experiments and, of course, higher than the negative control experiment performed on the C₁₁ monolayer (labeled as C in Figure 5). The fraction of aldehyde in the buried mixed monolayer can be calculated following the procedure employed for analysis of the TolA III-GFP protein data. By comparison of the N1s intensity measured for this low concentration with one of the three N1s core levels measured for higher aldehyde concentrations (100:0 10:90 and 5:95 C₁₀CHO:C₁₁), we obtained a value of $I_X/I_{100\%} = 0.21$. As the area of one PNA chain corresponds to the area occupied by 25.6 alkene chains, a 21% of PNA coverage corresponds to 0.8% of C₁₀CHO on the surface (0.8:99.2 C₁₀CHO:C₁₁).

The same result is obtained by analyzing the Si2p core level (data not shown here) instead of the N1s core level peaks. On the basis of the calculations performed by Petrovykh et al.⁴⁰⁻⁴² it is possible to determine the thickness of the close-packed biolayer as well as the aldehyde surface concentration for the partially covered silicon surface (for the most diluted aldehyde mixed monolayer). Petrovykh and co-workers determined how the attenuation of the substrate core level intensity, related to the presence of the biolayer, can be used to determine the layer thickness. These authors described a quantitative procedure for the characterization of DNA film thickness by XPS based on the electron attenuation effects of the substrate photoelectrons due to the presence of the biolayer (eq 1 in ref 40). By using this equation, modified for our system (our substrate core level

is the Si2p with an effective attenuation length, L_{Si} of the order of 2.1 nm^{41}), we estimate a ssPNA thickness of $t = 1.6 \text{ nm}$, in good agreement with the AFM images (see Figure 4). Therefore, XPS confirms that the molecules are lying down on the surface. We can consider now that the Si2p core level intensity measured for the partially covered surface is a combination of the silicon photoelectrons, which are attenuated only by the hydrocarbon layer, and those which are also attenuated by the PNA molecules

$$I_{Si} = XI_{Si}^0 \exp\left[-\frac{t}{L_{Si}}\right] + (1 - X)I_{Si}^0 \quad (1)$$

By use of the value of L_{Si} as before and the value of $t = 1.6 \text{ nm}$, we obtained $I_{Si(X)}/I_{Si(100\%)} = 0.19$, which again gives a value for the C₁₀CHO:C₁₁ ratio of 0.7%. Although slightly higher, the two results demonstrate that, within the experimental error, the ratio of reactive aldehyde groups to inert sites on the alkyl monolayer surface is close to the ratio in the preparation solution.

Therefore, by combination of structural information derived by AFM with the chemical specification and quantitative information provided by XPS, we have proved by different methods that the nominal value of aldehyde in the solution corresponds to the density of immobilized biomolecules supporting the chemical bonding between them and the surface.

The ability to control protein and nucleic acid immobilization by preparing dilute aldehyde layers is a useful alternative to nanoscale lithography.⁴³⁻⁴⁵ The monolayers prepared by reaction of mixture of alkene chains with the hydrogen terminated silicon surface present a homogeneous distribution of both components over the surface, and the composition is representative of the ratio of functional alkenes used in the solution reaction.^{16,17,21,46,47} In our experimental framework, this provides a convenient means to control the separation of reactive sites by a simple dilution method. These surfaces could be used for the development of biosensors as well as for several genomic and proteomic applications.

Conclusions

In conclusion, we present a direct and straightforward method to enable aldehyde functionalization of silicon surfaces suitable for Schiff base immobilization chemistry, without the need of protection group chemistry. Although aldehyde groups are known to react with hydrogen-terminated silicon, the difunctional vinyl aldehyde appears to react substantially via the vinyl end. Sufficient free, unreacted aldehyde groups remain intact for conjugation to proteins and PNA. The Schiff base formed by reaction of the lysine residues on proteins, as TolAIII-GFP, or the N-terminus of nucleic acids, as PNA, is reversible, although it can be fixed by reduction using NaCNBH₃ in a "one-pot" reaction in aqueous solution. We have determined that the number of biomolecules immobilized on very diluted (in terms of aldehyde content) modified surfaces is representative of the nominal ratio of the reactive aldehyde groups on the alkyl monolayer surface. Therefore, the reaction of the hydrogen-terminated silicon surface with the unprotected undecenyl aldehyde takes place mainly at the C=C under our thermal reaction conditions and forms a Si-C surface bond rather than a Si-O-C link. Because the reaction via the stable Si-C bond is irreversible and it is not directly influenced by the functional groups at the other end of the molecule, we are able to control the mean spacing between reactive groups on the surface by a simple dilution method. This represents a useful method for nanoscale surface design, suitable for the attachment of a broad range of biomolecules useful in biotechnological applications.

Acknowledgment. Work at Centro de Astrobiología was supported by European Union, Instituto Nacional de Técnica Aeroespacial, Spanish Ministry of Science (MEC), and Autonomous Community of Madrid. We acknowledge funding provided by MEC under Grant Nos. BIO2007-67523, MAT 2005-3866, and CSD 2007-41.

References and Notes

- (1) Zhang, S.; Marini, D. M.; Hwang, W.; Santoso, S. *Curr. Opin. Chem. Biol.* **2002**, *6*, 865.
- (2) Stoughton, R. B. *Annu. Rev. Biochem.* **2005**, *74*, 53.
- (3) Kumar, A.; Goel, G.; Fehrenbach, E.; Puniya, A. K.; Singh, K. *Eng. Life Sci.* **2005**, *5*, 215.
- (4) Park, H. G.; Song, J. Y.; Park, K. H.; Kim, M. H. *Chem. Eng. Sci.* **2006**, *61*, 954.
- (5) Drummond, T. G.; Hill, M. G.; Barton, J. K. *Nat. Biotechnol.* **2003**, *21*, 1192.
- (6) Briones, C.; Martín-Gago, J. A. *Curr. Nanosci.* **2006**, *2*, 257.
- (7) Vericat, C.; Vela, M. E.; Benítez, G. A.; Martín-Gago, J. A.; Torrelles, X.; and Salvezza, R. C. *J. Phys.: Condens. Matter* **2006**, *18*, R867.
- (8) Wang, H.; Tang, Z.; Li, Z.; Wang, E. *Surf. Sci.* **2001**, *480*, L389.
- (9) Briones, C.; Mateo-Martí, E.; Gómez-Navarro, C.; Parro, V.; Román, E.; Martín-Gago, J. A. *Phys. Rev. Lett.* **2004**, *93*, 208103.
- (10) Sasahara, A.; Uetsuka, H.; Ishibashi, T.; Onishi, H. *J. Phys. Chem. B* **2003**, *107*, 13925.
- (11) Terry, J.; Linford, M. R.; Wigren, C.; Cao, R.; Pianetta, P.; Chidsey, C. E. D. *J. Chem. Phys.* **1999**, *85*, 213.
- (12) Wu, C. R.; Nilsson, J. O.; Salaneck, W. R. *Phys. Scripta* **1987**, *35*, 586.
- (13) Linford, M. R.; Fenter, P.; Eisenberger, P. M.; Chidsey, C. E. D. *J. Am. Chem. Soc.* **1995**, *117*, 3145.
- (14) Buriak, J. M. *Philos. Trans. R. Soc. A* **2006**, *364*, 217.
- (15) Coffinier, Y.; Olivier, C.; Perzyna, A.; Grandidier, B.; Wallart, X.; Durand, J. O.; Melnyk, O.; Stievenard, D. *Langmuir* **2005**, *21*, 1489.
- (16) de Smet, L. C. P. M.; Zuilhof, H.; Sudholter, E. J. R.; Lie, L. H.; Houlton, A.; Horrocks, B. R. *J. Phys. Chem. B* **2005**, *109*, 12020.
- (17) de Smet, L. C. P. M.; Pukin, A. V.; Sun, Q. Y.; Eves, B. J.; Lopinski, G. P.; Visser, G. M.; Zuilhof, H.; Sudholter, E. J. R. *Carbohydr. Res.* **2004**, *339*, 2599.
- (18) Strother, T.; Cai, W.; Zhao, X. S.; Hamers, R. J.; Smith, L. M. *J. Am. Chem. Soc.* **2000**, *122*, 1205.
- (19) Strother, T.; Hamers, R. J.; Smith, L. M. *Nucleic Acids Res.* **2000**, *28*, 3535.
- (20) Lin, Z.; Strother, T.; Cai, W.; Cao, X. P.; Smith, L. M.; Hamers, R. J. *Langmuir* **2002**, *18*, 788.
- (21) Boukherroub, R.; Wayner, D. D. M. *J. Am. Chem. Soc.* **1999**, *121*, 11513.
- (22) Pike, A. R.; Lie, L. H.; Eagling, R. A.; Ryder, L. C.; Patole, S. N.; Connolly, B. A.; Horrocks, B. R.; Houlton, A. *Angew. Chem., Int. Ed.* **2002**, *41*, 615.
- (23) Pike, A. R.; Ryder, L. C.; Horrocks, B. R.; Clegg, W.; Connolly, B. A.; Houlton, A. *Chem.—Eur. J.* **2005**, *11*, 344.
- (24) Voicu, R.; Boukherroub, R.; Bartzoka, V.; Ward, T.; Wojtyk, J. T. C.; Wayner, D. D. M. *Langmuir* **2004**, *20*, 11713.
- (25) MacBeath, G.; Schreiber, S. L. *Science* **2000**, *289*, 1760.
- (26) Boukherroub, R.; Morin, S.; Sharpe, P.; Wayner, D. D. M.; Allongue, P. *Langmuir* **2000**, *16*, 7429.
- (27) Anderluh, G.; Gokce, I.; Lakey, J. H. *Prot. Exp. Pur.* **2003**, *28*, 173.
- (28) Nielsen, P. E.; Egholm, M.; Berg, R. H.; Buchardt, O. *Science* **1991**, *254*, 1497.
- (29) Egholm, M.; Buchardt, O.; Nielsen, P. E.; Berg, R. H. *J. Am. Chem. Soc.* **1992**, *114*, 1895.
- (30) Martínez, M. A.; Verdaguier, N.; Mateu, M. G.; Domingo, E. *Proc. Natl. Acad. Sci. USA.* **1997**, *94*, 6798.
- (31) Horcas, I.; Fernandez, R.; Gomez-Rodriguez, J. M.; Colchero, J.; Gomez-Herrero, J.; Baro, A. M. *Rev. Sci. Instrum.* **2007**, *78*, 013705.
- (32) Sun, Q.-Y.; de Smet, L. C. P. M.; van Lagen, B.; Giesbers, M.; Thune, P. C.; van Engelenburg, J.; de Wolf, F. A.; Zuilhof, H.; Sudholter, E. J. R. *J. Am. Chem. Soc.* **2005**, *127*, 2514.
- (33) Niederhauser, T. L.; Lua, Y.-Y.; Jiang, G.; Davis, S. D.; Matheson, R.; Hess, D. A.; Mowat, I. A.; Linford, M. R. *Angew. Chem., Int. Ed.* **2002**, *41*, 2353.
- (34) Huang, N. K.; Wang, D. Z.; Xiong, Q.; Yang, B. *Nucl. Instr. Meth. Phys. Res. B* **2003**, *207*, 395.
- (35) Wallart, X.; de Villeneuve, C. H.; Allongue, P. *J. Am. Chem. Soc.* **2005**, *127*, 7871.
- (36) Hong Q., Rogerio C., Lakey J. H., Horrocks B. R., Houlton A., Connolly B. A. In press.
- (37) Witty, M.; Sanz, C.; Shah, A.; Grossmann, J. G.; Mizuguchi, K.; Perham, R. N.; Luisi, B. *EMBO J.* **2002**, *21*, 4207. (a) Deprez, C.; Lloubès, R.; Gavioli, M.; Marion, D.; Guerlesquin, F.; Blanchard, L. *J. Mol. Biol.* **2005**, *346*, 1047.
- (38) Briones, C.; Mateo-Martí, E.; Gomez-Navarro, C.; Parro, V.; Roman, E.; Martín-Gago, J. A. *J. Mol. Catal. A: Chem.* **2005**, *228*, 131.
- (39) Mateo-Martí, E.; Briones, C.; Pradier, C. M.; Martín-Gago, J. A. *Biosens. Bioelectron.* **2007**, *22*, 1926.
- (40) Petrovykh, D. Y.; Kimura-Suda, H.; Tarlov, M. J.; Whitman, L. J. *Langmuir* **2004**, *20*, 429.
- (41) Kimura-Suda, H.; Petrovykh, D. Y.; Tarlov, M. J.; Whitman, L. J. *J. Am. Chem. Soc.* **2003**, *125*, 9014.
- (42) Lu, Z. H.; McCaffrey, J. P.; Brar, B.; Wilk, G. D.; Wallace, R. M.; Feldman, L. C.; Tay, S. P. *Appl. Phys. Lett.* **1997**, *71*, 2764.
- (43) Lim, J. H.; Ginger, D. S.; Lee, K. B.; Heo, J.; Nam, J. M.; Mirkin, C. A. *Angew. Chem., Int. Ed.* **2003**, *42*, 2309.
- (44) Sun, S. Q.; Chong, K. S. L.; Leggett, G. J. *J. Am. Chem. Soc.* **2002**, *124*, 2414.
- (45) Brewer, N. J.; Leggett, G. J. *Langmuir* **2004**, *20*, 4109.
- (46) de Smet, L.; Stork, G. A.; Hurenkarnp, G. H. F.; Sun, Q. Y.; Topal, H.; Vronen, P. J. E.; Sieval, A. B.; Wright, A.; Visser, G. M.; Zuilhof, H.; Sudholter, E. J. R. *J. Am. Chem. Soc.* **2003**, *125*, 13916.
- (47) Eves, B. J.; Sun, Q. Y.; Lopinski, G. P.; Zuilhof, H. *J. Am. Chem. Soc.* **2004**, *126*, 14318.